Journal of Biomolecular NMR **30:** 155–161, 2004.

Using chemical exchange to assign non-covalent protein complexes in slow exchange with the free state: Enhanced resolution and efficient signal editing

Juan Carlos Rodríguez[a], Patricia A. Jennings[a,*] & Giuseppe Melacini[b,*]
[a]*Department of Chemistry and Biochemistry, University of California San Diego, 9500 Gilman Dr., 92093-0359, La Jolla, U.S.A.;* [b]*Departments of Chemistry and Biochemistry, McMaster University, 1280 Main Street West, Hamilton, ON, Canada L8S 4M1*

Received 18 March 2004; Accepted 9 June 2004

Key words: assignments, chemical exchange, ligand binding, protein complexes

Abstract

The formation of a ligand-protein complex oftentimes results in significant chemical shift changes. These changes may occur not only in the binding pocket but also in distal regions of the protein target. Therefore the reassignment of the backbone resonances in the complex is frequently a time consuming challenge. Here we present a suite of resolution-enhanced N_z-exchange NMR experiments useful for rapidly assigning backbone ^1H and ^{15}N amide resonances of the ligand-bound form of a protein in slow exchange with its free state. Incorporation of semi-constant time frequency labeling periods into 3D N_z-exchange experiments in combination with the collection of resolution-enhanced 2D N_z-exchange difference spectra leads to a powerful set of tools for analyzing protein-ligand complexes. This allows for both the assignment of the bound state and the rapid assessment of the protein binding interface. The proposed methodology is demonstrated on the complex formed by the dimerization-docking domain of the c-AMP-dependent protein kinase and the tethering domain of the dual-binding A-kinase anchoring protein (AKAP).

Abbreviations: D-AKAP – Dual-binding A-kinase Anchoring Protein; D/D – Dimerization/Docking Domain; c-AMP – cyclic adenosin monophosphate; Ex. – exchange; C. Ex. – chemical exchange; NMR – nuclear magnetic resonance, PKA – c-AMP-dependent protein kinase, SCT – semi-constant time, RIα – regulatory subunit of type Iα PKA.

Introduction

Nuclear magnetic resonance (NMR) spectroscopy is ideally suited to characterize non-covalent interactions between macromolecules (Ikura et al., 1992; Qin et al., 2001; Zuiderweg, 2002). Among the simplest and most effective probes of such interactions are chemical shift changes occurring upon binding (McDonald and Phillips, 1967; Shuker et al., 1996; Foster et al., 1998). For instance, variations in chemical shifts observed in the presence of binding proteins are useful for mapping interaction surfaces (Foster et al., 1998; Qin et al., 2001; Zuiderweg, 2002). However, the NMR assignment of the bound state of a protein is often challenging either because of unfavorable relaxation properties owing to the increased size of the complex (Takahashi et al., 2000; Wüthrich, 2000) or because of extensive chemical shift variations caused by the binding induced conformational changes. Rather than the time-consuming process of the direct assignment of both the free and bound states of a protein, a more efficient strategy focuses first on the free state and then on the transfer of this assignment to the bound state. For instance, when the exchange between the free and

*To whom correspondence should be addressed. E-mail: melacin@mcmaster.ca, pajennin@chem.ucsd.edu

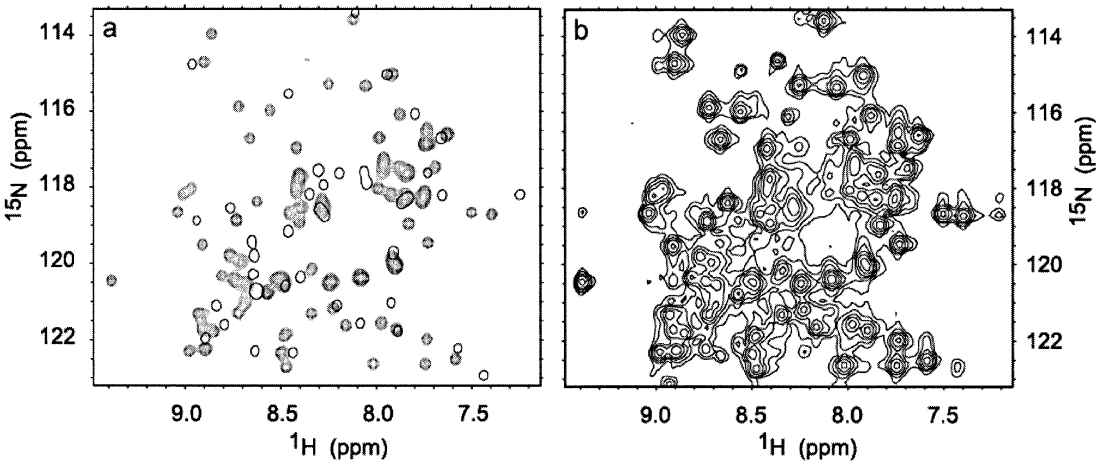

Figure 1. (a) Representative expansion of a ^{1}H-^{15}N HSQC spectrum of free RIα D/D (single contours) overlaid onto its D-AKAP2-bound state. (b) Same spectral region as in (a) but for a two-dimensional exchange spectrum (Vialle-Printems et al., 2000) of a sample containing ∼1 mM RIα D/D and 0.7 mM D-AKAP2 (333-359) peptide. Comparison of the spectra shown in panels (a) and (b) illustrates the crowding problem caused by the simultaneous presence of the free and the two bound resonance sets along with the exchange cross-peaks. Each resonance originating from free RIα D/D gives rise to two sets of resonances upon binding to the D-AKAP2 peptide as a result of the disruption of the two-fold symmetry in the dimer. Additional experimental details can be found in the Materials and methods section.

bound forms is slow in the chemical shift time scale, the assignment of the bound state can be obtained from that of the free state by transferring either longitudinal two spin order ($2I_zS_z$) or longitudinal ^{15}N magnetization (S_z) (Jeener et al., 1979; Montelione and Wagner, 1989; Wider et al., 1991; Farrow et al., 1994; Vialle-Printems et al., 2000). Since the auto relaxation rate is usually slower for S_z than for $2I_zS_z$, the experiments based on the S_z transfer allow the investigation of systems with a wider range of exchange rates (k_{off} in the $\sim 10 - 100\ s^{-1}$ range) (Vialle-Printems et al., 2000). One problem of the exchange experiments is that the free, bound and exchange cross-peaks are simultaneously present in the same spectrum, thus increasing the chance of peak overlap. This problem is exemplified by the case of the complex between the tethering domain of D-AKAP2 (Huang et al., 1997) and the dimerization/docking (D/D) domain (residues 12-61) of the RIα subunit of the cAMP-dependent protein kinase, PKA (Leon et al., 1997)α. The free RIα D/D domain possesses a C_2 axis of symmetry (Banky et al., 2000) so that the two monomers give rise to a single set of NMR resonances (Figure 1a). However, upon binding the non-palindromic D-AKAP2 peptide, this symmetry is lost and two sets of peaks are observed for the bound dimer (Figure 1a). The S_z-exchange spectrum for the RIα D/D in the presence of sub-stoichiometric amounts of D-AKAP2 peptide contains therefore auto peaks arising from the free and the two bound sets together with exchange cross-peaks among these three sets (Figure 1b). As a result, for each peak observed in the HSQC of the free RIα D/D there can be up to nine peaks in the exchange spectrum. In other words, the number of peaks in the exchange spectra can increase by almost one order of magnitude as compared to the simple HSQC spectrum of the free state, resulting in extremely crowded spectra (Figure 1b). It is therefore important to design experiments that deconvolute this spectral complexity not only by increasing the dimensionality of the exchange spectra (Vialle-Printems et al., 2000), but also by optimizing the resolution. In this paper, we propose a pair of 3D S_z-exchange experiments in which the resolution is enhanced through the extensive use of semi-constant time frequency labeling (Figure 2) (Grzesiek and Bax, 1993; Logan et al., 1993). In addition, we also designed a 2D difference (Wider et al., 1991) semi-constant time S_z-exchange pulse sequence that separates exchange cross-peaks from overlapping auto-peaks (Figure 4). This set of resolution-enhanced and edited S_z-exchange experiments is expected to facilitate the assignment of macromolecular complexes.

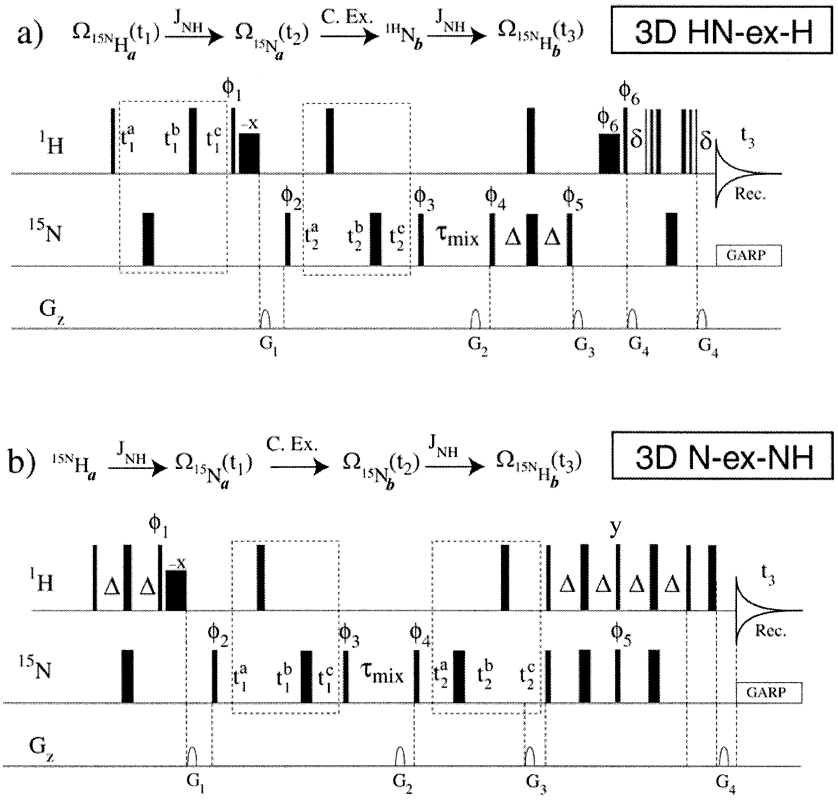

Figure 2. Pulse sequences for the semi-constant time 3D-HN-ex-H (**a**) and for the semi-constant time gradient and sensitivity-enhanced 3D-N-ex-NH (**b**) experiments. Semi-constant time evolution periods are highlighted by the dashed boxes. Narrow and wide bars represent 90° and 180° pulses, respectively, whereas lower and larger rectangles indicate the water-flip back pulses. All pulses have 'x' phase unless otherwise indicated. The delay Δ is set to $1/4J = 2.75$ ms, whereas τ_{mix} defines the exchange mixing time. (a) The semi-constant time incremented delays for the t_1 dimension are: $t_{1a} = \Delta + 3\ \mu s + [m/(2SW_1)]$, $t_{1b} = 3\ \mu s + [(0.5/SW_1) - (\Delta/M)]m$, and $t_{1c} = p180N + 6\ \mu s + \Delta - (\Delta/M)m$, where p180N is the duration of the ^{15}N 180° pulse, SW_1 is the spectral width for the F1 dimension and $m = 0, 1, ..., M - 1$ ($t_1 = m/SW_1$). $M$is the total number of complex t_1 points. Similarly, the semi-constant time incremented delays for the t_2 dimension are: $t_{2a} = \Delta + 3\ \mu s + [n/(2SW_2)]$, $t_{2b} = 3\ \mu s + [(0.5/SW_2) - (\Delta/N)]n$, and $t_{2c} = p180H + 6\ \mu s + \Delta - (\Delta/N)n$, where p180H is the duration of the ^1H 180° pulse, SW_2 is the spectral width for the F2 dimension and $n = 0, 1, ..., N - 1$ ($t_2 = n/SW_2$). $N$is the total number of complex t_2 points. The water suppression is achieved through the 3-9-19 WATERGATE scheme with the delay δ set accordingly to (Piotto et al., 1992). The phase cycle is: ϕ_1 = y, y, −y, −y; ϕ_2 = x, −x; ϕ_3 = y, −y, −y, y, y, −y, −y, y, −y, y, y, −y, −y, y, y, −y; ϕ_4 = x, -x, x, −x, x, −x, x, −x, −x, x, −x, x, −x, x, −x, x; ϕ_5 = y, y, −y, −y; ϕ_6 = x, x, x, x, −x, −x, −x, −x; rec. = x, −x, −x, x, −x, x, x, −x. The relative gradient strengths are: G_{1x}: 0, G_{1y}: 0, G_{1z}: 1.00; G_{2x}: 0, G_{2y}: 2.75, G_{2z}: 2.75; G_{3x}: 3.88, G_{3y}: 0, G_{3z}: 3.88; G_{4x}: 2.13, G_{4y}: 2.13, G_{3z}: 1.59. (b) The semi-constant time incremented delays for the t_1 dimension of the 3D-N-ex-NH experiment are the same as the corresponding delays for the t_2 dimension of the 3D-HN-ex-H experiment in panel (a). The semi-constant time incremented delays for the t_2 dimension of the 3D-N-ex-NH experiment are: $t_{2a} = p180H + 6\ \mu s + \Delta - (\Delta/N)n$, $t_{2b} = 3\ \mu s + [(0.5/SW_2) - (\Delta/N)]n$ and $t_{2c} = \Delta + 3\ \mu s + [n/(2SW_2)]$, where p180H is the duration of the ^1H 180° pulse, SW_2 is the spectral width for the F2 dimension and $n = 0, 1, ..., N - 1$ ($t_2 = n/SW_2$). As before, N is the total number of complex t_2 points. The phase cycle for the 3D-N-ex-NH pulse sequence is: ϕ_1 = y, y, −y, −y; ϕ_2 = x, −x; ϕ_3 = y, y, y, y, −y, −y, −y, −y; ϕ_4 = 8(x), 8(−x), rec. = x, −x, −x, x, −x, x, x, −x, −x, x, x, −x, x, −x, −x, x. The phase ϕ_5 is y and it is inverted synchronously with the sign of the ^{15}N-encoding gradient G3 to achieve Echo/Anti-Echo quadrature detection for t_2. The relative gradient strengths in the 3D-N-ex-NH experiment are: G_{1x}: 0, G_{1y}: 0, G_{1z}: 1.00; G_{2x}: 0, G_{2y}: 2.75, G_{2z}: 2.75; G_{3x}: +/− 6.88, G_{3y}: +/− 6.88, G_{3z}: +/− 5.16; G_{4x}: 0.688, G_{4y}: 0.688, G_{3z}: 0.516. Additional experimental details can be found in the Materials and methods section.

Materials and methods

Sample preparation

The dimerization/docking (D/D) domain of ^{15}N-labeled RIα (residues 1-61) was expressed in *Escherichia coli* Rossetta (DE3) (Novagen) and purified by Ni^{2+} affinity and size exclusion chromatographies (Banky et al., 2000). Fragment (12–61) of RIα was prepared by trypsin digestion as reported previously (Banky et al., 2000). The unlabeled tethering domain (residues 333–359) of D-AKAP2 (Ac-VQGNDEAQEELAWKIAKMIVSDVMQQ-NH2)

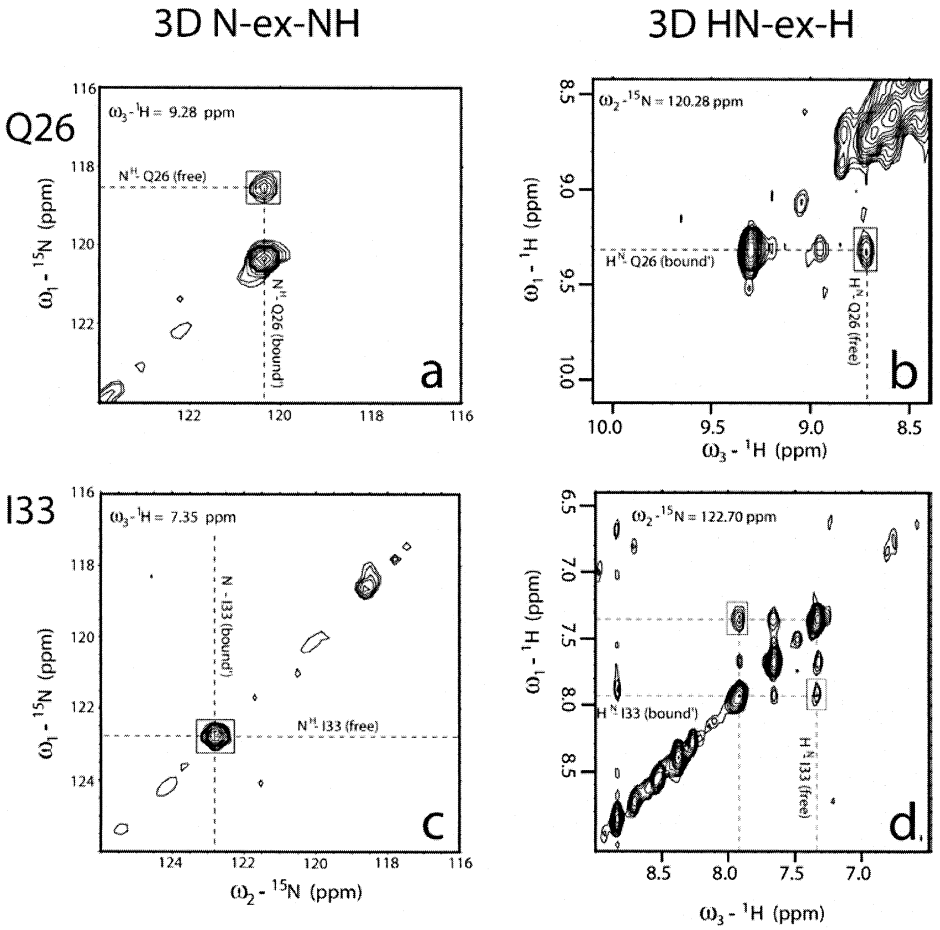

Figure 3. Representative 3D-N-ex-NH and 3D-HN-ex-H cross-peaks for Q26 (panels a and b) and I33 (panels c and d), respectively. The notation 'bound' 'refers to one of the two bound resonance sets. For Q26 the bound' and the free resonances have distinct chemical shifts along both the ^{1}H and the ^{15}N dimensions so that in both 3D spectra (a and b) the exchange cross-peaks are well resolved from the diagonal. For I33 the bound' and the free resonances have very similar ^{15}N chemical shifts so that the free-bound' cross-peak for I33 is resolved in the 3D-HN-ex-H spectrum (d) but not in the 3D-N-ex-NH spectrum (c). Exchange cross-peaks are boxed within rectangles or squares. Additional experimental details can be found in the Materials and methods section.

was synthesized by Anaspec (San Jose, CA). The RIα D/D / D-AKAP2 complex (1:1 stoichiometry) was prepared by addition of a weighed amount of lyophilized peptide into ∼10 mL of RIα D/D solutions (50 mM sodium acetate, 100 mM sodium chloride, pH 4.0). The complex was purified from the free protein and/or peptide by gel filtration chromatography (Sephacryl S-100). Fractions containing pure RIα D/D / D-AKAP2 complex were pooled and concentrated to approximately 500 μL with the aid of ultrafiltration membranes (3000 Da MWCO). NMR samples were prepared by adding enough sodium azide and D_2O to these solutions to achieve a final concentration of 0.02% and 10%, respectively. The RIα D/D / D-AKAP2 complex gives good spectra under these experimental conditions. However, the *free* D-AKAP2 (333–359) peptide is insoluble under the conditions necessary for our studies of the complex. In addition, the peptide can dissociate during the course of the acquisition of the NMR data. Thus, the 1:1 complex is metastable under these conditions owing to the aggregation of the D-AKAP2 (333–359) peptide in its free state. In order to circumvent this problem, we prepared **sub**-stoichiometric mixtures of RIα D/D and D-AKAP2. Peptide rebinding to the excess free RIα D/D, rather than peptide aggregation, is favored under these conditions and the integrity of the sample is maintained. The concentration of protein in the free form was estimated by comparison of peak intensities in ^{1}H-^{15}N HSQC spectra taken immediately

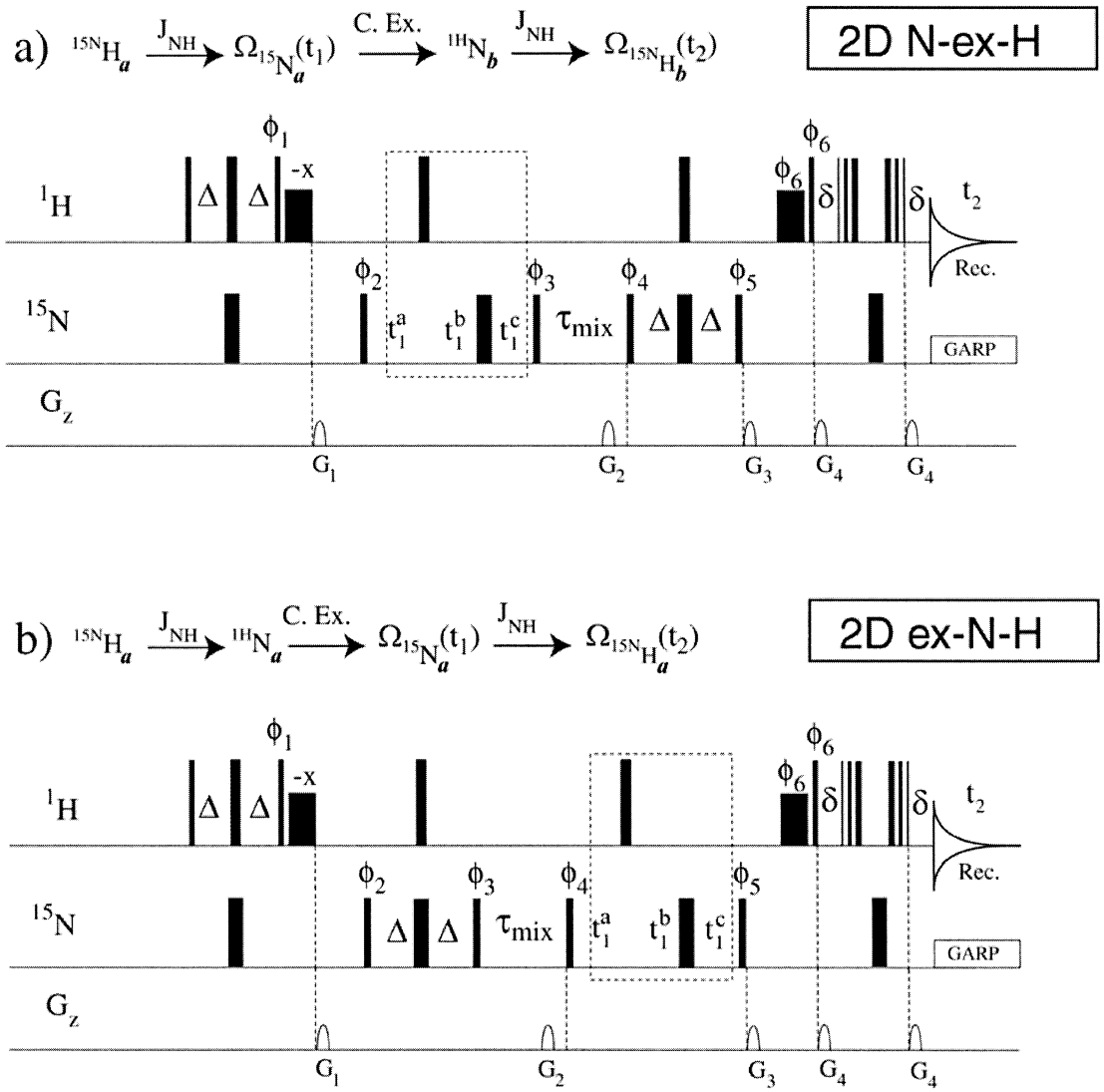

Figure 4. Pulse sequences for the semi-constant time 2D-N_z exchange difference experiment. Semi-constant time evolution periods are highlighted by the dashed boxes. The 2D N-ex-H (a) and the 2D ex-N-H (b) were acquired in interleaved mode in order to minimize difference artifacts. All fixed delays, pulse symbols, phase cycles and gradient strengths are as for the 3D HN-ex-H experiment (Figure 2a). The semi-constant time variable delays for the t_1 dimension are as in the 3D N-ex-NH experiment (Figure 2b). Additional experimental details can be found in the Materials and methods section.

after sample preparation and just before acquisition of the exchange spectra. The concentration of protein in the 1:1 complex was estimated by the method of Gill and von Hippel (Gill and von Hippel, 1989) using extinction coefficients of 6090 M^{-1} cm^{-1} and 5400 M^{-1} cm^{-1} at 276 nm for the dimeric RIα D/D and for the D-AKAP2 peptide, respectively.

NMR experiments

All NMR spectra were acquired using the same experimental conditions: temperature of 308 K, pH 4.0, 50 mM sodium acetate, 100 mM NaCl. The 2D-N-ex-H-differenence and the 3D-N-ex-NH spectra were acquired at 600 MHz (Bruker DRX spectrometer), while the remaining spectra were acquired at 500 MHz (Bruker DMX spectrometer). The ^{15}N decoupling was implemented in all experiments using the GARP sequence (Shaka et al., 1985) with an RF field strength

of 1 or 1.25 kHz. All water-flip back pulses had a rectangular shape and duration of 2 ms. Quadrature detection was achieved using the States-TPPI method (Marion et al., 1989) for all indirectly detected dimensions except for t_2 of the 3D N-ex-NH experiment in Figure 2b in which the Echo/Anti-echo approach was used (Schleucher et al., 1993). The ^{1}H carrier frequency was on the water signal whereas that for ^{15}N was at the center of the amide region. All gradients were sine-bell shaped with duration of 0.8 ms and a ring-down delay of at least 0.2 ms. The exchange mixing time was 230 ms in all experiments. The relaxation delay between transients was at least 1.1 s for all pulse sequences. For all the ^{15}N dimensions the spectral width was 1317.78 Hz and 64 complex points were acquired. For all the directly detected ^{1}H dimensions the spectral width was 8389.26 Hz and 512 complex points were recorded. In the indirectly detected H^N dimension of the 3D-HN-ex-H spectrum 50 complex points were acquired for a spectral width (SW_1) of 2999.94 Hz. Additional information can be found in the figure captions.

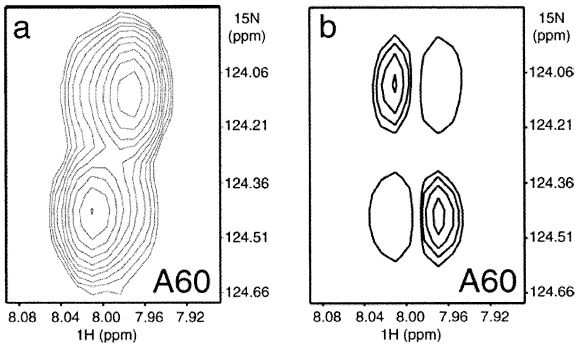

Figure 5. Representative expansions of the cross-peaks for A60 in the spectrum acquired with the pulse sequence of Figure 4a (a) and in the semi-constant time 2D-N_z exchange difference experiment (b). The two bound A60 sets coincide and their resonances significantly overlap with those of free A60 both along the ^{1}H and the ^{15}N dimensions. As a result in the unedited exchange spectrum (a) the exchange cross-peaks for A60 cannot be resolved; however these cross-peaks are clearly detected in the difference experiment (b). Negative peaks were plotted with only one contour line and result from the difference between auto-peaks. Additional experimental details can be found in the Materials and methods section.

Results and Discussion

As shown in Figure 1b, the complexity of unedited 2D-exchange spectra presents a challenge even for relatively small protein-protein complexes, such as the RIα/D / D-AKAP2 (333–359) system. However, significant simplification of the exchange spectra can be obtained by combining increased dimensionality (3D) (Vialle-Printems et al., 2000) with semi-constant time frequency labeling (Grzesiek and Bax, 1993; Logan et al., 1993). Specifically, two semi-constant time 3D-exchange experiments are proposed: a 3D HN-ex-H pulse sequence, in which both ^{1}H and ^{15}N spins are frequency labeled before the exchange mixing time (Figure 2a), and a 3D N-ex-NH, in which only ^{15}N spins are frequency labeled before the exchange mixing time (Figure 2b). The key differences between the 3D experiments proposed here and those of Vialle-Printems (Vialle-Printems et al., 2000) are the extensive application of semi-constant time frequency labeling and of sensitivity enhancement when applicable. In the 3D HN-ex-H pulse sequence the semi-constant time evolution of ^{1}H and ^{15}N chemical shifts takes advantage of the INEPT and refocused-INEPT delays necessary to create $^{15}N_z$ magnetization before the exchange mixing period (Figure 2a), whereas in the 3D-N-ex-NH experiment the semi-constant time evolution of ^{15}N chemical shifts uses also the delay of the dephasing INEPT that immediately follows the mixing block. In all cases the simultaneous chemical shift and scalar coupling evolution implemented through the semi-constant time schemes scales down the signal decay caused by relaxation. In the case of the 3D-N-ex-NH experiment it is also possible to implement echo/anti-echo quadrature detection with sensitivity enhancement, as shown in Figure 2b (Sattler et al., 1999).

The combined analysis of the semi-constant time 3D-N-ex-NH and 3D HN-ex-H experiments is very useful to reliably assign exchange cross-peaks. For instance, when the exchange is between two states with well resolved frequencies in both the ^{1}H and the ^{15}N dimensions, such as the case of Q26, then the exchange cross-peaks are observed in both 3D spectra (Figures 3a, b) providing an independent validation of the assignment of the cross-peak. However, when the exchange is between two states with well resolved frequencies only in the ^{1}H or the ^{15}N dimensions, then the exchange cross-peak is observed only in one of the two 3D spectra. For example, the backbone resonance frequencies for I33 in the free and one of the bound states are characterized by different ^{1}H frequencies but very similar ^{15}N chemical shifts. In this case, no exchange cross-peak is detectable in the 3D-N-ex-NH spectrum (Figure 3c) but a clear exchange cross-peak appears in the 3D-HN-ex-H spectrum (Fig-

ure 3d). Similarly, for cases in which the exchanging peaks are well resolved only in the ^{15}N dimension, the exchange cross-peaks are observed in the 3D-N-ex-NH experiment but not in the 3D-HN-ex-H data set.

When the exchange is between two states with poorly resolved frequencies in both the ^{1}H and the ^{15}N dimensions, then the exchange cross-peak resides very close to the diagonal of both 3D-N-ex-NH and 3D-HN-ex-H spectra and therefore none of the pulse sequences of Figure 2 is suitable. For these poorly resolved cases, a 2D-difference experiment (Wider et al., 1991) was designed (Figure 4) in which the semi-constant time ^{15}N frequency labeling occurs alternatively before (2D N-ex-H pulse sequence in Figure 4a) or after (2D ex-N-H pulse sequence in Figure 4b) the exchange mixing period. Both 2D N-ex-H and 2D-ex-NH pulse sequences detect the auto-peaks but only the 2D N-ex-H experiment allows the observation of exchange-cross peaks. As a result the difference spectrum (2D N-ex-H – 2D-ex-N-H) contains greatly reduced auto-peaks that facilitate the observation of the exchange-cross peaks. For instance, for A60 the free and bound resonances are so poorly resolved along both the ^{1}H and the ^{15}N dimensions that it is not possible to separate the auto-peaks from the exchange cross-peaks in the unedited spectrum (Figure 5a). However, in the semi-constant time $^{15}N_z$-exchange difference experiment this separation is easily achieved (Figure 5b). Even if the auto-peaks are dramatically attenuated, they are still present in the difference spectrum but with opposite sign relative to the exchange cross-peaks (Figure 5b). This is because the absence of exchange cross-peaks in the 2D-ex-N-H spectrum makes its auto-peaks more intense than the corresponding auto-peaks in the 2D-N-ex-H spectrum.

In conclusion, the combination of 2D and 3D $^{15}N_z$-exchange experiments with semi-constant time frequency labeling and with difference spectroscopy resulted in a suite of resolution-enhanced $^{15}N_z$-exchange pulse sequences that facilitates the assignment of exchanging systems, such as the free and bound states of a protein.

Acknowledgements

The authors wish to thank Dr John M. Wright for expert NMR assistance. This work was supported by grant DK54441 from the National Institutes of Health. Financial support from the W. M. Keck Foundation for computing resources at the W.M. Keck Laboratory for Integrated Biology II is gratefully acknowledged.

References

Banky, P., Newlon, M.G., Roy, M., Garrod, S., Taylor, S.S. and Jennings, P.A. (2000) *J. Biol. Chem.*, **275**, 35146–35152.

Farrow, N.A., Zhang, O.W., Forman-Kay, J.D. and Kay, L.E. (1994) *J. Biomol. NMR*, **4**, 727–734.

Foster, M.P., Wuttke, D.S., Clemens, K.R., Jahnke, W., Radhakrishnan, I., Tennant, L., Reymond, M., Chung, J. and Wright, P.E. (1998) *J. Biomol. NMR*, **12**, 51–71.

Gill, S.C. and von Hippel, P.H. (1989) *Anal. Biochem.*, **189**, 319–326.

Grzesiek, S. and Bax, A. (1993) *J. Biomol. NMR*, **3**, 185–204.

Huang, L.J.S., Durick, K., Weiner, J.A., Chun, J. and Taylor, S.S. (1997) *Proc. Natl. Acad. Sci. U.S.A.*, **94**, 11184–11189.

Ikura, M., Clore, G.M., Gronenborn, A.M., Zhu, G., Klee, C.B. and Bax, A. (1992) *Science*, **256**, 632–638.

Jeener, J., Meier, B.H., Bachmann, P. and Ernst, R.R. (1979) *J. Chem. Phys.*, **71**, 4546–4553.

Leon, D.A., Herberg, F.W., Banky, P. and Taylor, S.S. (1997) *J. Biol. Chem.*, **272**, 28431–28437.

Logan, T.M., Olejniczak, E.T., Xu, R.X. and Fesik, S.W. (1993) *J. Biomol. NMR*, **3**, 225–231.

Marion, D., Ikura, M., Tschudin, R. and Bax, A. (1989) *J. Magn. Reson.*, **85**, 393–399.

McDonald, C.C. and Phillips, W.D. (1967) *J. Am. Chem. Soc.*, **89**, 6332–6341.

Montelione, G. and Wagner, G. (1989) *J. Am. Chem. Soc.*, **111**, 3096–3098.

Piotto, M., Saudek, V. and Sklenar, V. (1992) *J. Biomol. NMR*, **2**, 661–666.

Qin, J., Vinogradova, O. and Gronenborn, A.M. (2001) *Meth. Enzymol.*, **339**, 377–389.

Sattler, M., Schleucher, J. and Griesinger, C. (1999) *Prog. NMR Spectrosc.*, **34**, 93–158.

Schleucher, J., Sattler, M. and Griesinger, C. (1993) *Angew. Chem. Int. Ed. Engl.*, **32**, 1489–1491.

Shaka, A.J., Barker, P.B. and Freeman, R.J. (1985) *J. Magn. Reson.*, **64**, 547–552.

Shuker, S.B., Hajduk, P.J., Meadows, R.P. and Fesik, S.W. (1996) *Science*, **274**, 1531–1534.

Takahashi, H., Nakanishi, T., Kami, K., Arata, Y. and Shimada, I. (2000) *Nat. Struct. Biol.*, **7**, 220–223.

Vialle-Printems, C., van Heijenoort, C. and Guittet, E. (2000) *J. Magn. Reson.*, **142**, 276–279.

Wider, G., Neri, D. and Wüthrich, K. (1991) *J. Biomol. NMR*, **1**, 93–98.

Wüthrich, K. (2000) *Nat. Struct. Biol.*, **7**, 188–189.

Zuiderweg, E.R.P. (2002) *Biochemistry*, **41**, 1–7.